High-precision Pb and Hf isotope and highly siderophile element abundance systematics of high-MgO Icelandic lavas

Robert W. Nicklas[1], Alan D. Brandon[2], Tod E. Waight[3], Igor S. Puchtel[4], James M. D. Day[1]

[1]Scripps Institution of Oceanography, University of California San Diego, La Jolla, CA 92093, USA

[2]Earth and Atmospheric Sciences Department, University of Houston, Houston, TX 77204, USA

[3]Department of Geosciences and Natural Resource Management (Geology Section), University of Copenhagen, Copenhagen K, Denmark

[4]Department of Geology, University of Maryland, College Park, MD 20742, USA

Corresponding author:

Robert William Nicklas; e-mail: rwnicklas@ucsd.edu

To be submitted to:

Chemical Geology

6,548 Words, 66 References, 3 Tables, 8 Figures

Version 2020/04/09

Abstract

Ocean island basalts (OIB) are well known to exhibit significant variations in their $^{87}Sr/^{86}Sr$, $^{143}Nd/^{144}Nd$, $^{176}Hf/^{177}Hf$, $^{186,187}Os/^{188}Os$, and $^{206,207,208}Pb/^{204}Pb$ compositions relative to chondrites. In order to further constrain the relationship between diverse long-lived isotopic systems in OIB, new double-spike Pb and Hf isotope data, as well as highly siderophile element (HSE: Os, Ir, Ru, Pt, Pd, and Re) abundances are reported for nineteen Icelandic picrites and basalts for which $^{3}He/^{4}He$, $^{87}Sr/^{86}Sr$, $^{143}Nd/^{144}Nd$, and $^{186,187}Os/^{188}Os$ data have been reported previously (Brandon et al., 2007. *GCA*). Hf-Nd isotope systematics of the sample set reveal the presence of an ancient refractory source with low-$^{3}He/^{4}He$, while He-Pb isotope correlations indicate that recycled oceanic crustal components with high-$^{3}He/^{4}He$ added from a less degassed mantle source are present in the source of the Iceland plume. The highly depleted, low-$^{3}He/^{4}He$ signature is sampled in the Northern and Western Volcanic Zones, likely due to higher degrees of partial melting at those localities enabling sampling of this refractory endmember. Osmium isotope ratios show correlations with Pb, Hf, and Nd isotope ratios indicating binary mixing between depleted and enriched sources, with no evidence for decoupling due to sulfide metasomatism. The spread of $^{187}Os/^{188}Os$- $^{206,207,208}Pb/^{204}Pb$ data can be explained by mixing of 1-11% young recycled oceanic crust into a depleted mantle source distinct from the source of Atlantic MORB. Abundances of the HSE in Northern and Western Volcanic Zone lavas overlap with those from other OIB with similar MgO contents, showing fractionated patterns enriched in the incompatible Re, Pd, and Pt over compatible Ru, Ir, and Os. Calculated parental melt HSE abundances of those lavas also overlap with those of other OIB. Eastern Volcanic Zone lavas are highly depleted in Pt and Pd relative to other Icelandic lavas. Abundances of Pt and Pd correlate with isotopic parameters, such as $^{206}Pb/^{204}Pb$, in Icelandic lavas, indicating that the isotopically enriched endmember sampled in the Eastern Volcanic Zone is depleted in the HSE, consistent with it being mafic in nature. The abundance of MgO in the lavas also roughly

correlate with isotopic parameters, supporting the identity of the depleted endmember as ultramafic and the enriched endmember as mafic. New and previously published double-spike Pb isotope data show chiefly binary mixing with an additional component present in the vicinity of the volcano Öræfajökull. Icelandic $^{207}Pb/^{204}Pb$ and $^{208}Pb/^{204}Pb$ data plot below and above the northern hemisphere reference line, respectively, indicating that both depleted and enriched end-members in the plume have a lower U depletion age and a higher Th/U than ambient northern hemisphere mantle. This is consistent with the enriched and depleted end-members within the Iceland plume being <2 Ga recycled oceanic crust and lithospheric mantle, respectively.

1. Introduction:

Ocean island basalts (OIB) are generally thought to be the result of melting in deep-seated high temperature mantle plumes (e.g., Hoffman, 1997). OIB are distinct from mid-ocean ridge basalts (MORB) in terms of their incompatible trace element abundances and long- and short-lived isotope systems, including Rb-Sr, Sm-Nd, Lu-Hf, U-Th-Pb, Re-Pt-Os, and Hf-W (e.g., Zindler and Hart, 1984; Salters and White, 1998; Brandon et al. 1998; Day et al. 2013; Mundl et al. 2017). Specifically, OIB show a much wider range of isotopic compositions than global MORB, varying between at least four major isotopic endmembers: high-μ (HIMU) with radiogenic Pb and MORB-like Sr, but low Nd and Hf isotopic ratios; enriched mantle 1 (EM1) and enriched mantle 2 (EM2), both showing varying degrees of radiogenic Sr and unradiogenic Nd and Hf, as well as unradiogenic Pb (EM1), or radiogenic Pb (EM2); and the focal zone (FOZO), primordial helium mantle (PHEM), or common (C) component that represents a ^{3}He-enriched mantle reservoir with intermediate Nd, Sr, Hf, and Pb isotope compositions that is long-term incompatible trace element depleted with respect to the bulk silicate Earth (Hart et al., 1992; Farley et al., 1992; Hanan & Graham, 1996; Jackson et al., 2020).

Although large amounts of high-quality OIB isotopic data are available in the literature, currently lacking are studies that report Nd, Hf, Sr, Pb, and Os isotopic data on the same samples. This is important for constraining the relationship of these systems to one another in the terrestrial mantle. The U-Th-Pb isotope system is an especially powerful geochemical tool, as Pb has three radiogenic isotopes and, therefore, mixing lines in Pb-Pb plots are straight lines, making identifying diverse endmembers relatively straightforward. The Lu-Hf isotope system offers a powerful means of identifying ancient deep melting processes, as Lu is highly compatible in garnet and deep garnet-residual melting will decouple the normally strongly correlated Lu-Hf and Sm-Nd isotope systems (Stracke et al., 2003). As Hf isotope data were not systematically collected for OIB before the late 1990s (i.e. Blichert-Toft et al., 1999), data for this isotope system are relatively limited compared to Nd or Sr. Similarly, Os isotope data acquisition requires specialized digestion and separation techniques, leading to relatively few labs reporting Os isotope data for OIB (Day, 2013). Although the isotopic compositions of OIB endmembers are now considered to have largely been defined, relatively few studies have reported the full suite of isotope data for the same samples, limiting information on the behavior of these systems relative to one another.

Iceland is a prominent example of a deep-seated plume located on a ridge axis and shows a much larger isotopic range than the adjacent Mid-Atlantic ridge (Hemond et al. 1993; Thirlwall, 1995; 1997; Fitton et al. 1997; Kempton et al. 2000; Chauvel and Hemond, 2000; Fitton et al. 2003; Thirlwall et al. 2004; Kokfelt et al. 2006; Brandon et al. 2007; Peate et al. 2010; Koornneef et al. 2012). Modern Icelandic lavas chiefly erupt in three main rift zones: the Northern Volcanic Zone (NVZ), Eastern Volcanic Zone (EVZ), and Western Volcanic Zone (WVZ), all of which exude relatively primitive lavas (Shorttle and Maclennan, 2011). Iceland is notable for erupting higher-MgO tholeiitic lavas compared to typical OIB, generally held to be the result of higher degrees of partial melting caused by the

combination of a high-temperature plume mantle with the thin lithosphere at the ridge axis. The lack of older oceanic crust or continental materials make Icelandic (and other OIB) lavas susceptible to edifice contamination (e.g., Condomines et al., 1983; Macpherson et al., 2005), but not to modification of long-lived radiogenic isotopic compositions (Brandon et al., 2007). Available oxygen isotopic data also argue against significant contamination by seawater or meteoritic water in Icelandic basalts (Thirlwall et al. 2006).

In order to constrain the relationship between different isotope systems within the Icelandic plume, new Hf and double-spike Pb isotopic systematics and isotope dilution HSE (Os, Ir, Ru, Pt, Pd, and Re) abundances are reported for a suite of Icelandic high MgO lavas, for which Tl, Nd, Sr, He and $^{186\text{-}187}$Os isotopic systematics have previously been published (Brandon et al., 2007; Nielsen et al., 2007; Debaille et al., 2009). Given the available isotopic and the major and trace element concentration data (Brandon et al. 2007; Nielsen et al. 2007), this sample set is now among the most comprehensively described of all Icelandic sample sets and, thus, can be used to constrain the relationships between different geochemical variables in the Iceland plume.

2. Sample Set Background

All picrite and basalt samples were collected for the purpose of studying the Os isotopic systematics of the Icelandic plume (Brandon et al., 2007). Therefore, the samples were collected to have high MgO (9.5 to 28.5 wt.%) and, thus, high Os contents (0.083 to 1.41 ppb) for high-precision ^{186}Os/^{188}Os analyses, as well as to contain olivine phenocrysts, in order to conduct He isotope analyses. Samples cover all three major rift zones in Iceland, with two picrites from the NVZ, three picrites from the EVZ and twelve picrites and two basalts from the WVZ. Bulk rock major element abundances, ^{186,187}Os/^{187}Os and ^{143}Nd/^{144}Nd compositions, and Re and Os abundances have been reported in the

studied samples by Brandon et al. (2007), along with $^{3}He/^{4}He$ ratios measured for olivine separates. $^{87}Sr/^{86}Sr$ data for the sample set are reported in the appendices of Debaille et al. (2009). Trace element abundances in the olivine crystals have been reported for a subset of the samples, and these data constrain the oxygen fugacity of three of the WVZ picrites (ICE-4A, ICE-4B, and ICE-5) to be close to that of MORB (Nicklas et al., 2019). Finally, bulk rock trace element abundances and stable Tl isotopic systematics of the sample set have been reported by Nielsen et al. (2007).

Picrites from the EVZ are enriched in incompatible trace elements and show elevated chondrite-normalized La/Sm ratios of ~1.7-1.8, likely indicating lower degrees of melting than for the other samples (0.31-1.7, majority <0.7). All the samples are olivine-rich and many of them are texturally consistent with olivine accumulation. Bulk rock MgO contents vary between 9.5 and 28.5 wt.% and bulk rock Mg# varies between 0.61 and 0.86. The samples show negligible variation in $^{186}Os/^{188}Os$ or $^{205}Tl/^{203}Tl$ ratios, indicating that the presence of either outer core metal, or pelagic sediment in the Iceland plume mantle was undetectable (Brandon et al. 2007; Nielsen et al. 2007). The Nd, Os, and He isotopic data show variable mixing between a depleted, low-$^{3}He/^{4}He$ endmember and a more enriched high-$^{3}He/^{4}He$ endmember that may represent recycled oceanic crust recharged with primordial He in the lower mantle (Brandon et al., 2007). Alternatively, this enriched endmember may be early differentiated, less degassed material, associated with all deep-seated high-$^{3}He/^{4}He$ plumes as the "FOZO" endmember (Jackson et al., 2020). Older Icelandic lavas host some of the highest-$^{3}He/^{4}He$ known to exist on Earth (>40 R_A; Hilton et al. 1999), whereas younger Icelandic volcanic rocks and geothermal fluids sample a mantle source with somewhat lower $^{3}He/^{4}He$ (up to 20-25 R_A; e.g., Hardardottir et al., 2018). These relationships demonstrate that some amount of primordial, less degassed component is sampled by the plume. The identity of the depleted end-member in Icelandic lavas has variably been identified as recycled lithospheric mantle intrinsic to the Iceland plume (Chauvel and Hemond, 2000; Fitton et al.,

2003), or local MORB mantle mixed with a small amount of enriched plume component (Hanan et al., 2000). The new Hf, Pb, and HSE data reported here offer further constraints as to the identity of these endmembers.

3. Analytical Methods:

The Pb and Hf isotope analyses were performed at the Danish Lithosphere Centre in Copenhagen, Denmark. Lead isotopic analyses were done on hand-picked rock chips leached in hot 7 M HCl for ~1 hour. Chips were then washed repeatedly with ultrapure Milli-Q water. The ^{207}Pb-^{204}Pb double spike method of Baker et al. (2004) was then applied to the cleaned chips. In brief, the rock chips were digested in a sequence of HF/HNO_3 followed by HCl, and then Pb was isolated by standard HBr column chromatography. Two analyses were made of all Pb aliquots, the first without and the second with the ^{207}Pb-^{204}Pb double spike added. Total procedural blanks were 16-44 pg Pb and were negligible compared to the amount of Pb in the digested sample aliquots.

Hafnium was separated from whole rock powders using the flux fusion and column chromatography method of Ulfbeck et al. (2003). Total procedural Hf blanks were <100 pg and were, therefore, also negligible. Both Pb and Hf were run using an *Cetac* Aridus de-solvating nebulizer connected to an *Axiom* multi-collector inductively-coupled plasma mass spectrometer (MC-ICP-MS) at the Danish Lithosphere Centre. Replicate analyses of SRM981 over the course of the study gave ^{206}Pb/^{204}Pb = 16.9408 ± 0.0014, ^{207}Pb/^{204}Pb = 15.4987 ± 0.0019 and ^{208}Pb/^{204}Pb = 36.7230 ± 0.0043 (n = 13). Replicate analyses of the in-house DLC Hf standard gave ^{176}Hf/^{177}Hf = 0.281872 ± 0.000022 (n = 6) (all errors 2SD). Hafnium isotopic analyses were normalized to an in-house standard ^{177}Hf/^{176}Hf ratio of 0.28189, which is equivalent to 0.28216 for JMC475.

Abundances of the HSE (Os, Ir, Ru, Pt, and Pd) in whole rock samples and olivine and chromite separates from sample ICE-4A were determined at The University of Chicago following the protocol of Puchtel et al. (2004) by isotope dilution using inverse aqua regia Carius tube digestion with a mixed HSE spike at 250˚C for 96 hrs, followed by anion exchange chromatography for Ir, Ru, Pt, and Pd. Osmium was extracted from the aqua regia solution using CCl_4 solvent extraction and purified using HBr microdistillation and measured by thermal ionization mass spectrometry. The HSE abundances were determined using a single-collector *ThermoFisher* Element 2 inductively-coupled mass-spectrometer. The long-term reproducibility of in-house HSE standard solutions was better than 2% for all elements. For additional details on the analytical techniques used to determine the HSE abundances the reader is also referred to Puchtel and Humayun (2005).

4. Results

The new Pb and Hf isotopic data are reported in **Table 1.** The $^{206}Pb/^{204}Pb$, $^{207}Pb/^{204}Pb$, $^{208}Pb/^{204}Pb$ ratios range between 18.048 and 18.967, 15.432 and 15.518, 37.711 and 38.526, respectively, and $\varepsilon^{176}Hf$ values ($\varepsilon^{176}Hf = 10{,}000* ((^{176}Hf/^{177}Hf)_{t,\ sample}/(^{176}Hf/^{177}Hf)_{t,\ CHUR} - 1)$ range between +11.6 and +20.7. These new data are well within the range of data for Icelandic lavas available from the *Georoc* database. The $\varepsilon^{176}Hf$ and $\varepsilon^{143}Nd$ values (calculated using the CHUR values of Bouvier et al. 2008) are plotted against each other in **Figure 1**, along with the Hf-Nd isotope mantle array of Vervoort and Blichert-Toft (1999) and previously reported Icelandic data (Kempton et al. 2000; Stracke et al. 2003; Peate et al. 2010). The data scatter above the mantle array to higher $\varepsilon^{176}Hf$ values at the depleted end of the dataset, which is dominated by the WVZ and NVZ picrites.

In **Figure 2**, $^{3}He/^{4}He$ ratios are plotted against the new bulk-rock $^{206}Pb/^{204}Pb$, $^{208}Pb/^{204}Pb$, and $^{176}Hf/^{177}Hf$ ratios. These data show broad positive correlations between the He and Pb isotope ratios and

a negative correlation between the He and Hf isotope ratios. The most Hf isotope 'depleted' samples have the lowest $^{3}He/^{4}He$. Lithophile element isotopic ratios are plotted against $^{187}Os/^{188}Os$ in **Figure 3**, with broad positive correlations with Pb isotope ratios and negative correlations with Nd and Hf ratios. Strontium isotope ratios scatter and show no correlation with Os isotopes. Lead isotope ratios are plotted against each other in **Figure 4**, along with the northern hemisphere reference line (NHRL) of Hart (1984). Both $^{208}Pb/^{204}Pb$ and $^{207}Pb/^{204}Pb$ show strong positive correlations with $^{206}Pb/^{204}Pb$, with the $^{208}Pb/^{204}Pb$ data plotting above the NHRL, and the $^{207}Pb/^{204}Pb$ data below it.

Abundances of the HSE are listed in **Table 2**, and primitive mantle (PM) normalized abundances are plotted in **Figure 5a**. All samples show enrichments in PM-normalized Re, Pt, and Pd abundances relative to Ru, Ir, and Os, consistent with data for other OIB (Day, 2013). The HSE concentrations in the olivine separate of ICE-4A are largely lower than those in the bulk rock (**Figure 5b.**), while the chromite separate from the same sample is enriched in Os, Ir, Ru, and Pt and depleted in Pd relative to the bulk rock sample. The $D^{chromite/bulk}$ values vary between 0.73 (Pd) and 76 (Ru) and $D^{olivine/bulk}$ values vary between 0.04 and 1.27. Abundances of the HSE are also plotted against bulk rock MgO contents in **Supplemental Figure 1**, showing a broad positive correlation for Os, Ir, and Ru, a broad negative correlation for Re, and no discernable correlation for Pt and Pd.

5. Discussion

5.1 Hafnium-Neodymium isotope systematics:

Given the breadth of isotopic systems now analyzed for the same bulk-rock samples (i.e., He, Sr, Nd, Hf, $^{187,186}Os$, Pb, Tl), the new dataset offers an opportunity to examine the behavior of different isotopic signatures relative to one another in rocks that show clear trends between strongly depleted and less depleted sources in Iceland. In **Figure 1**, anomalous behavior is notable in that the majority of NVZ

and EVZ picrites plot above the Nd-Hf mantle array, indicating Nd-Hf decoupling in their mantle source regions (Stracke et al. 2003). The parameter ΔεHf, defined as the vertical deviation in epsilon units from the mantle array, ranges from -1.8 to +4.7, roughly positively correlating with ε^{143}Nd, indicating that the more LREE-depleted samples plot furthest away from the mantle array (**Table 1**). The Hf-Nd isotope mantle array is defined by the relative incompatibilities of Sm, Nd, Lu, and Hf during mantle melting and even modest deviations require explanation. Such decoupling has been previously observed in Icelandic lavas (Stracke et al. 2003), Hawaiian OIB (Blichert-Toft et al. 1999), mid-ocean ridge basalts north of Iceland (Blichert-Toft et al. 2005) and, most commonly, in mantle peridotites (Bizimis et al. 2003; 2005; Stracke et al. 2011). This decoupling is also a common feature in some early Archean komatiites, such as those from the Barberton Greenstone Belt (Puchtel et al., 2013; 2016), and disappears in their late Archean counterparts.

Two main scenarios have been proposed to explain such Nd-Hf isotopic decoupling in OIB: incorporation of zircon-poor pelagic sediment into the mantle (i.e., Blichert-Toft et al. 1999) and decoupling of Hf from Nd at high degrees of deep garnet-residual melting in ancient, depleted mantle lithologies (i.e., Bizimis et al. 2003; Stracke et al. 2011). It is unlikely that the NVZ and EVZ picrites incorporated pelagic sediment in their source regions due to their depleted Nd isotope systematics (εNd up to +10) and their MORB-like $^{206}Pb/^{204}Pb$ ratios (18.048 to 18.887), both highly uncharacteristic of ancient subducted pelagic sediments that have εNd values of <-5.9 and $^{206}Pb/^{204}Pb$ ratios of <17.467 (Eisele et al. 2002). Incorporation of pelagic sediments would also lead to large variations in ε^{205}Tl, which are not observed in the sample set (Nielsen et al. 2007). These picrites – particularly those from the NVZ and WVZ – can therefore be assumed to sample a highly depleted peridotite endmember similar to the abyssal peridotites reported by Stracke et al. (2011). Such an end-member may be

volumetrically major in the Iceland source mantle, but its low Nd and Hf concentrations relative to more fertile mantle lithologies and its refractory nature makes it a minor component in isotope variation diagrams of the lavas. Indeed, it has recently been suggested that such ultra-depleted domains may be ubiquitous in the upper mantle but under-recognized due to the low amounts of melt they produce relative to less depleted mantle sources (Stracke et al. 2019). This scenario has also been proposed using Os isotope data (Day, 2013).

Assuming that the most depleted sample, 9809, represents this depleted endmember, the endmember is characterized by a ε^{143}Nd of 9.5, a ε^{176}Hf of 20.7, ^{206}Pb-^{207}Pb-^{208}Pb/^{204}Pb of 18.3684, 15.4715 and 38.0646 respectively, and a ^{187}Os/^{188}Os of 0.1308. Such an endmember shows Pb marginally more radiogenic than the "ID1" endmember of Thirlwall et al. (2004) with ^{206}Pb-^{207}Pb-^{208}Pb/^{204}Pb of 17.87, 15.42 and 37.53, likely because of the smaller dataset examined in this study. The presence of elevated mantle temperatures and thin lithosphere underlying Iceland means that highly depleted components are more readily sampled here than in other plumes, especially along the WVZ and NVZ, where high degrees of partial melting are evident (Shorttle and Maclennan, 2011).

5.2 Correlation of helium and other isotope systems

It is well-established that Icelandic lavas can have elevated ^{3}He/^{4}He ratios of up to 20 - 25 R_A, well above North Atlantic MORB at ~8 ± 1 R_A (Kurz et al. 1985; Hilton et al. 1999; Macpherson et al. 2005; Brandon et al. 2007; Hardarsdottir et al. 2018). Noble gas data provide some of the most important lines of evidence for a deeply sourced mantle plume being present beneath Iceland. Elevated ^{3}He/^{4}He ratios are concentrated in modern basalts from central and eastern Iceland, consistent with the center of the plume being present there (Kurz et al. 1985; Macpherson et al., 2005; Hardarsdottir et al., 2018). Our sample set shows no such correlation with geography (**Figure 2**), possibly as a result of the

relatively low number of samples for which He isotope data are available. The data do, however, show a positive correlation between radiogenic Pb isotopes and $^{3}He/^{4}He$, and a negative correlation between radiogenic Hf isotopic composition and $^{3}He/^{4}He$. These correlations are perhaps counter-intuitive, as radiogenic Pb is produced by the decay of U and Th, both of which also produce ^{4}He. However, the association of high-$^{3}He/^{4}He$ with enriched isotopic compositions is not uncommon in OIB lavas (i.e., Ellam and Stuart, 2004) and has been previously recognized using the $^{187}Os/^{188}Os$-$^{3}He/^{4}He$ correlations within the sample set (Brandon et al. 2007). Higher $^{3}He/^{4}He$ correlated with radiogenic Pb is also observed in OIB from Hawaii (Eiler et al. 1998) and Cape Verde (Doucelance et al. 2003). Consistent with their highly melt depleted and degassed nature, the high $\Delta\varepsilon Hf$, high $^{176}Hf/^{177}Hf$ lavas from the NVZ and WVZ plot with the lowest $^{3}He/^{4}He$ (Fig. 2). In agreement with Brandon et al. (2007), we invoke two stage mixing, in which a subducted package of lithosphere (crust and sediments) mixed with a high-$^{3}He/^{4}He$ component in the lower mantle before being entrained in the plume and mixed with the depleted Iceland-endmember, which is distinct from global MORB (Thirlwall et al. 2004). It is unlikely that the less degassed endmember is a primordial endmember such as "FOZO" (Jackson et al. 2020) due to its Pb isotope systematics (high $\Delta^{208}Pb$ and low $\Delta^{207}Pb$, Table 1). Given the likely low He-concentrations of subducted materials and their low calculated $^{3}He/^{4}He$ ratios (Day et al., 2015), mixing with only a small amount of a high He concentration, high-$^{3}He/^{4}He$ mantle component is necessary. Therefore this component is not evident in other isotopic systems. An alternative model postulates that the high-$^{3}He/^{4}He$ Icelandic endmember is an early formed, never homogenized reservoir that is characterized by low-$\delta^{18}O$ and is unrelated to recycled oceanic crust (Thirlwall et al. 2006). This scenario is unlikely given the enriched nature of the less degassed endmember with high $^{3}He/^{4}He$ (**Figure 2**) which strongly supports a recycled crust origin.

5.3 Correlation of Long-Lived Isotope Systems:

Rhenium and Os are highly siderophile and chalcophile elements that are hosted in minor phases in mantle lithologies, with Os also being highly compatible during mantle melting. These properties can make correlation between Os isotopic signatures and lithophile element isotopic signatures complex (Day, 2013). Conversely, good correlations are observed in the current sample set (**Figure 3**) as $^{187}Os/^{188}Os$ compositions show broad positive correlations with Pb isotope ratios and broad negative correlations with Nd and Hf isotopes, indicating that lithophile and siderophile/chalcophile isotope systems behave coherently in the Iceland plume. The sample set shows uniform $^{186}Os/^{188}Os$ and $^{205}Tl/^{203}Tl$ ratios and, thus, no correlation is shown between these ratios and other isotopic data (**Supplemental Figure 2**). It is notable, however, that Os and Sr isotopic systematics also show no correlation with one another (**Figure 3**). Although it is possible that the scatter in Sr isotopes is the result of assimilation of altered rocks within the volcanic edifice, this is inconsistent with oxygen isotopic systematics of Icelandic lavas (Thirlwall et al. 2006). Those authors concluded that more than two endmembers are necessary to explain Icelandic Sr isotope systematics, but that all other isotope systems only show two dominant endmembers.

The coherent behavior of Nd, Hf, Pb, and Os isotopes in the high MgO lavas studied here show that two component mixing can explain the bulk of the variation in modern Icelandic lavas. This is consistent with the previous principle component analysis (PCA) calculations that showed that mixing between two end-members can explain 99% of the isotopic variations of Icelandic lavas (Peate et al. 2010). Similar conclusions have been reached for basalts from the adjacent Reykjanes and Kolbeinsey ridges (Blichert-Toft et al. 2005). The high $^{206,207,208}Pb/^{204}Pb$, high $^{187}Os/^{188}Os$, low $^{143}Nd/^{144}Nd$, $^{176}Hf/^{177}Hf$ endmember is likely recycled oceanic crust, consistent with previous conclusions regarding Icelandic lavas (Chauvel and Hemond, 2000; Brandon et al. 2007; Koornneef et al. 2012). Two of the

four endmembers of Thirlwall et al. (2004), the enriched "IE1" and the depleted "ID1", encompass the entire range of Pb, Sr, and Nd data for our sample set, and are thus potentially viable endmembers. The $^{206\text{-}207\text{-}208}Pb/^{204}Pb$ compositions of these endmembers, along with Pb concentrations of 0.03 ppm (ID1) and 0.45 ppm (IE1) were used with $^{187}Os/^{188}Os$ and Os concentrations of 0.125 and 2.81 ppb (ID1) and 2.0 and 0.15 ppb (IE1), respectively, to test simple bulk mixing models. The Pb and Os concentrations and the $^{187}Os/^{188}Os$ ratio in the endmembers were selected to be similar to recycled crust (IE1) and depleted oceanic lithospheric mantle (ID1), while the Pb isotopic compositions were taken from Thirlwall et al. (2004). The results of these model calculations are presented in **Supplemental Figure 3** and show that mixing ~1-11% of IE1 with bulk ID1 can explain the spread data. The success of such simple models indicate that the main Icelandic isotopic endmembers can be viably explained by incorporating a single package of recycled oceanic lithosphere. High-$^{3}He/^{4}He$ associated with the enriched endmember IE1 indicates it originates from deep in the mantle.

As Re and Os are chiefly hosted in minor sulfide phases in mantle peridotites, they can potentially be decoupled from other isotope systems by migration of sulfide liquids within the mantle (Luguet et al. 2008). This evidently did not occur within the Iceland plume. The high-degree melting in the hot low-pressure melting zone beneath Iceland may have effectively homogenized any potential small-scale heterogeneities, leading to the relatively simple two-component mixing that is observed. Alternatively, migration of sulfide liquids over sufficient time-scales to result in long-term Os isotopic variations (i.e. Waters et al., 2020), did not occur. It is likely that the depleted end-member ID1 is not ambient North Atlantic depleted mantle but instead a depleted component intrinsic to the Iceland plume (Fitton et al. 2003; Thirlwall et al. 2004), as demonstrated by its low $^{207}Pb/^{204}Pb$ at a given $^{206}Pb/^{204}Pb$ (**Figure 4**).

5.4 Highly Siderophile Element Abundances in Iceland

The newly reported data overlap entirely with the HSE data reported previously for Icelandic lavas (Rehkämper et al. 1999; Momme et al. 2003) as shown in **Supplemental Figure 4**. Much of the previous HSE abundance data was obtained using lower precision methods, such as the Ni-sulfide fire assay technique, and the data presented here are the highest precision isotope dilution HSE dataset yet reported for Icelandic lavas. The HSE CI-normalized patterns are indistinguishable between samples from the NVZ and the WVZ (**Figure 5**), while EVZ lavas are systematically depleted Pd and Pt relative to the other lavas. Processes such as fractional crystallization, crustal assimilation, and differential partial melting can strongly affect the concentrations of HSE in an erupted magma (Barnes et al., 1985). The elements Os, Ir and Ru are strongly compatible during mantle melting in OIB systems, while Pt, Pd, and Re are moderately incompatible (Day et al. 2013). Similarly, during sulfide undersaturated fractional crystallization, Os, Ir and Ru behave compatibly while Pt, Pd and Re behave incompatibly (Barnes et al. 1985; Rehkämper et al. 1999). The HSEs are all strongly compatible in sulfide phases, but primitive Icelandic volcanic zone lavas are unlikely to have ever saturated a sulfide phase (Momme et al. 2003). Despite the potentially strong effects of differential partial melting and fractional crystallization, the abundances of the HSE still show rough correlations with isotopic parameters, such as $^{206}Pb/^{204}Pb$ (**Figure 6**). Isotopic compositions cannot be modified by partial melting or fractional crystallization and therefore must reflect source variations. The data shown in **Figure 6a.** indicate that the endmember with radiogenic Pb (i.e. oceanic crust) is depleted in Pd relative to the unradiogenic Pb endmember. The radiogenic EVZ lavas are seemingly sampling this HSE depleted source. Interestingly, bulk rock MgO content is also roughly correlated with $^{206}Pb/^{204}Pb$ (**Figure 6b.**), as well as with $^{176}Hf/^{177}Hf$. Although MgO content is also strongly affected by degree of partial melting and fractional crystallization, it is still apparent in the dataset that the isotopically enriched endmember is lower in

MgO than the depleted endmember, consistent with its identity as mafic material. Such a mixing trend in major element abundances and HSE abundances is relatively rarely observed in oceanic lavas (i.e., Day et al. 2013). Its preservation in the Iceland dataset attests to the primitive, minimally fractionated nature of the erupted lavas as well as the high degrees of melting present beneath Iceland accessing even refractory lithologies within the plume.

Although HSE abundances show only weak correlations with MgO (**Supplemental Figure 1**), likely due to the effects of fractional crystallization and olivine accumulation, these rough correlations can be used to estimate the HSE content of an average parental lava. Previous work used olivine major element systematics in the sample suite to estimate that the average parental magma had ~17.9 wt.% MgO (Nicklas et al. 2019). Using linear correlations between MgO and each HSE, a calculated parental magma contained approximately 0.67 ± 0.27 ppb Os, 0.31 ± 0.14 ppb Ir, 1.1 ± 0.3 ppb Ru, 5.2 ± 4.2 ppb Pt, 10.4 ± 10.3 ppb Pd and 0.44 ± 0.32 ppb Re. Uncertainties on these estimates are the 95% confidence intervals of the regressions. The total abundance of all the HSE in this theoretical parental magma is 17.7 ppb, close to the average total HSE concentration for the sample set of 16.6 ppb, indicating that the cumulate lavas contain much of the HSE and dominate the average. The parental magma HSE patterns of the olivine and chromite separates can also be estimated using the empirically determined HSE partition coefficients of Puchtel and Humayun (2001). The HSE concentrations of the three calculated parental magmas are listed in **Table 3** and are plotted in **Figure 7a.** The three calculated parental magmas overlap well with each other, given the uncertainties in the partition coefficients, indicating that they are a good estimate for the average parental HSE composition, as all three were determined using independent methods. The HSE concentrations of the Icelandic parental magmas overlap with the range of calculated parental magmas of lavas from major Hawaiian volcanoes (Ireland et al. 2011), Azorean volcanoes (Waters et al. 2020) and Western Canary Islands volcanoes (Day et al. 2010) (**Figure 7b.**).

The average EVZ lava HSE pattern is also shown in **Figure 7**. This pattern is depleted relative to the three parental lava patterns, especially in Pt and Pd. This fact, coupled with the correlation of Pd concentration with isotopic parameters, such as $^{206}Pb/^{204}Pb$ (**Figure 6a.**), indicates that HSE abundances were controlled by mixing between the two endmembers, along with secondary effects of fractional crystallization processes. This is consistent with the relative compatibility of the HSE during mantle melting, leaving an isotopically depleted peridotite enriched in HSE. These data also indicate that the high $^{3}He/^{4}He$ endmember is relatively poor in the HSE, which are highly enriched in the Earth's core, meaning that relationships between the HSE and a theoretical high-$^{3}He/^{4}He$ signature from the core (i.e., Porcelli and Halliday, 2001) are not straightforward to interpret (Brandon et al., 2007).

5.5 Lead Isotope Systematics of Icelandic Lavas:

Similar to the parameter $\Delta\varepsilon Hf$, $\Delta^{207}Pb$ and $\Delta^{208}Pb$ are the vertical deviations of $^{207}Pb/^{204}Pb$ and $^{208}Pb/^{204}Pb$ from the NHRL (Hart, 1984). Eighteen of the nineteen samples show negative $\Delta^{207}Pb$ and sixteen of the nineteen samples show positive $\Delta^{208}Pb$ (**Table 1**), plotting below and above the NHRL, respectively (**Figure 4**). The highly depleted samples with high $\Delta\varepsilon Hf$ do not show extreme $\Delta^{207}Pb$ or $\Delta^{208}Pb$, plotting near the average values. The $^{206}Pb/^{204}Pb$-$^{207}Pb/^{204}Pb$ and $^{206}Pb/^{204}Pb$-$^{208}Pb/^{204}Pb$ NHRLs are expressions of the average age at which U/Pb was set and of the average time-integrated Th/U ratio in the northern hemisphere oceanic mantle, respectively (Hart 1984). The predominantly negative $\Delta^{207}Pb$ values show that Icelandic mantle has a younger U/Pb age than average mantle, as has been previously proposed (Thirlwall, 1997; Thirlwall et al. 2004). This indicates that the high $^{3}He/^{4}He$-$^{206}Pb/^{204}Pb$ component beneath Iceland did not form early, unlike the theoretical reservoir "FOZO" (Jackson et al. 2020). As both the depleted and enriched Icelandic end-members show negative $\Delta^{207}Pb$, it is evident that neither of them can be ambient entrained mantle. This inferred young age indicates the presence of

relatively young (<2 Ga) recycled lithosphere in the plume, consistent with conclusions from Os isotope systematics (Brandon et al. 2007). Previously reported Pb isotope systematics suggest a younger recycling age of ~170 Ma (Thirlwall et al. 1997; Thirlwall et al. 2004), but Os isotopic data require a recycling age of >1.5 Ga, and it is unlikely that crust could be recycled and re-entrained in a deep plume in <170 Ma. Alternatively, the isotope systems could date mantle metasomatism that formed the enriched endmember.

The positive Δ^{208}Pb values show that the Icelandic plume mantle has elevated Th/U compared to ambient mantle, again consistent with its origin as recycled lithosphere. Thorium is much less fluid-mobile during subduction than U, and both oceanic crust and underlying lithospheric mantle can develop elevated Th/U during subduction-related dehydration (Kelley et al., 2005). It should be noted that the more radiogenic samples show systematically lower Δ^{208}Pb, indicating that the samples with the highest U/Pb also show low Th/U, consistent with a smaller loss of U during subduction in that end of the sample array (**Figure 4**). Therefore, the depleted and enriched endmembers can be explained by a single package of recycled oceanic lithosphere, as argued by Chauvel and Hemond (2000). Because Pb is the daughter element of three separate decay systems, it is an excellent isotope system to distinguish the number of end-members in a system, as all mixing arrays will be straight lines. The presence of a high-^{3}He/^{4}He endmember (**Figure 2**) requires a relatively less degassed source deep in the mantle, as He is not efficiently recycled into the mantle. The newly reported Pb isotope systematics reinforce the conclusion that the lavas can be broadly explained by binary mixing between depleted and enriched endmembers with only a minor amount of scatter (**Figure 4**).

There have been numerous Pb isotopic data published for modern Icelandic lavas (Thirlwall et al. 2004; Kokfelt et al. 2006; Peate et al. 2009; 2010; Manning and Thirlwall, 2014), but only data obtained using the Pb double-spike technique were plotted in **Figure 4** for consistency, as other Pb

isotopic data may not be accurate or precise (Thirlwall, 2002; Baker et al. 2004) and the large amount of available data for Iceland allows for such filtering while still maintaining large datasets. The new Pb data are entirely within the range of previously reported double-spike Pb data. Mixing in Pb isotope space will result in linear trends and while the conclusion of binary mixing is broadly consistent with the expanded Pb isotope dataset, the situation is clearly more complex. Thirlwall et al. (2004) modelled Pb isotope systematics in Iceland in detail and identified four different endmembers, including two enriched and two depleted components (Figure 4). In addition to the main trend, a trend is seen towards an endmember with elevated $^{207}Pb/^{204}Pb$ and $^{208}Pb/^{204}Pb$ at intermediate $^{206}Pb/^{204}Pb$ (**Figure 4**) The elevated $\Delta^{207}Pb$ and $\Delta^{208}Pb$ endmember is only evident in the EVZ in the vicinity of the volcano Öræfajökull. Öræfajökull erupts among the most isotopically enriched lavas in Iceland, trending towards the global end-member "EM2" (Prestvik et al. 2001). The Öræfajökull endmember is proposed to be ambient plume mantle mixed with 0.5% recycled sediment (Prestvik et al. 2001; Manning and Thirlwall, 2014). Such a signature would likely be easily recognizable using Tl isotope systematics, as that system is sensitive to small additions of high Tl sediments (Nielsen et al. 2007), although more recent OIB Tl data contradict this conventional wisdom (Brett et al. 2021). Alternatively, geophysical evidence suggests that a sliver of continental crust may be present beneath Southeast Iceland and 2-6% contamination of mantle melts by such crust could lead to the observed compositions of the Öræfajökull lavas (Torsvik et al 2015). Unfortunately, neither Os nor O isotopic data are currently available for Öræfajökull lavas, and new data will serve to illuminate the identity of this endmember as either recycled pelagic sediment or continental crust contamination. The majority of reported Icelandic double-spike Pb data have both negative $\Delta^{207}Pb$ and positive $\Delta^{208}Pb$, with 66% of the 179 data points having both these properties (**Figure 8**). This shows that the bulk of the Icelandic basalts sample a source with a young U-depletion age and an elevated Th/U, consistent with the recycled lithosphere model. The Pb

isotopic endmembers of Thirlwall et al. (2004) are plotted in **Figures 4** and **8**, but it is evident that these endmembers do not encompass the entire range of the data, especially the Öræfajökull endmember.

6. Conclusions:

New Pb and Hf isotopic data and highly siderophile element abundances (HSE) are reported for nineteen picrites and basalts from the three main Neovolcanic zones of Iceland for which $^{186\text{-}187}$Os, Nd, Sr, He, and Tl isotopic data have previously been published. The Nd-Hf data for the sample set show strong correlation, the depleted end of which plots above the mantle array, indicating the involvement of a highly depleted refractory mantle in the source of the NVZ and WVZ picrites. Such a refractory depleted source is likely tapped by the combination of high temperatures and thin lithosphere present in the Icelandic volcanic zones. The high-^{3}He/^{4}He endmember in Iceland is characterized by radiogenic Pb and Os, likely as a result of high U/Pb-Re/Os recycled oceanic crust mixing with a less-degassed deep mantle reservoir with high He concentrations in the deep mantle, consistent with previous models (i.e., Brandon et al., 2007). Osmium isotopic systematics correlate with Nd, Hf, and Pb in the sample set, showing broad-scale binary mixing in the Iceland source between depleted and enriched mantle components, although more detailed Pb isotope studies indicate that multiple depleted and enriched components may be involved. The observed binary mixing can be modeled as addition of 1-11% of enriched endmember "IE1" to depleted endmember "ID1" from Thirlwall et al. (2004). The coherency of Os with lithophile isotope systems shows that sulfide metasomatism is not a significant process in the Iceland plume mantle. The HSE abundances in the Iceland lavas overlap with those in the Hawaiian lavas with similar MgO contents, possibly indicating similar HSE abundances in the Icelandic and Hawaiian plumes. Parental magma compositions of WVZ and NVZ lavas show HSE abundances overlapping with parental abundances in other OIB, such as Hawaii. Lavas from the EVZ are highly

depleted in Pt and Pd relative to the other samples, probably due to depletion in HSE in their mantle source region. Abundances of Pt, Pd, and MgO show broad correlations with isotopic parameters, such as $^{206}Pb/^{204}Pb$ and $^{176}Hf/^{177}Hf$, indicating that their abundances are controlled by source mixing and not simply by crystal-liquid fractionation. These correlations indicate that the isotopically enriched endmember is likely mafic in composition and is depleted in HSE and that the depleted endmember is ultramafic in composition and is higher in HSE. This observation is consistent with the enriched endmember being recycled oceanic crust. The new and published data show consistently negative $\Delta^{207}Pb$ and positive $\Delta^{208}Pb$ across both depleted and enriched samples. The Iceland source probably consists of a depleted recycled mantle lithosphere and an enriched recycled oceanic crust both depleted in U by dehydration during subduction. In line with previous studies (i.e. Peate et al. 2010), we conclude that two end-members dominate the isotopic variation in Icelandic lavas. The third, more minor end-member is only found in the vicinity of the Öræfajökull volcano in the EVZ. Future O, Os and Tl isotope studies of lavas from this volcano could illuminate whether this endmember is recycled sediment or continental crust buried within the Icelandic volcanic edifice.

7. Acknowledgements:

Joel Baker is thanked for his leadership and guidance in the DLC Axiom MC-ICPMS laboratory. Fieldwork to gather the sample set was funded by NSF EAR Grant 0000908 to A.D.B.

Table 1: Lead and Hf isotopic ratios of bulk rock Icelandic basalts and picrites. Abbreviations: Northern Rift Zone Picrite – NVZ, Eastern Rift Zone Picrite – EVZ, Western Rift Zone Picrite – WVZ Pic and Western Rift Zone Basalt – WVZ Bas. Sample locations in Brandon et al. (2007).

	$^{206}Pb/^{204}Pb$	2s	$^{207}Pb/^{204}Pb$	2s	$^{208}Pb/^{204}Pb$	2s	$^{176}Hf/^{177}Hf$	2s	Location	$\Delta^{207}Pb$	$\Delta^{208}Pb$	εHf	ΔHf
Ice0	18.2040	0.0021	15.4471	0.0019	37.8764	0.0048	0.283327	0.000007	NRZ	-1.73	24.1	15.7	3.83
Ice2	18.4987	0.0024	15.4680	0.0021	38.1325	0.0050	0.283318	0.000008	WRZ Pic	-2.83	14.1	19.6	2.80
Ice3	18.8865	0.0007	15.5110	0.0006	38.4674	0.0017	0.283148	0.000006	WRZ Pic	-2.73	0.66	15.9	0.71
Ice4A	18.4880	0.0016	15.4666	0.0016	38.1233	0.0039	0.283276	0.000007	WRZ Pic	-2.85	14.4	20.7	2.50
Ice4b	18.4883	0.0016	15.4659	0.0015	38.1251	0.0037	0.283263	0.000006	WRZ Pic	-2.92	14.6	14.6	2.11
Ice5	18.5381	0.0023	15.4835	0.0021	38.2161	0.0052	0.283239	0.000007	WRZ Pic	-1.70	17.7	18.7	2.22
Ice6	18.0475	0.0011	15.4321	0.0010	37.7112	0.0025	0.283286	0.000005	NRZ	-1.53	26.5	14.3	2.86
Ice8a	18.9575	0.0009	15.5115	0.0008	38.5185	0.0020	0.283127	0.000006	ERZ	-3.45	-2.81	19.6	-1.09
Ice8b	18.9667	0.0007	15.5117	0.0007	38.5259	0.0018	0.283144	0.000006	ERZ	-3.53	-3.19	16.3	-0.40
Ice9a	18.9424	0.0017	15.5103	0.0007	38.5000	0.0017	0.283101	0.000006	ERZ	-3.41	-2.83	17.6	-1.79
Ice10	18.7878	0.0015	15.4969	0.0013	38.3648	0.0032	0.283232	0.000006	WRZ Pic	-3.07	2.33	19.3	2.25
Ice11	18.4062	0.0023	15.4963	0.0022	38.1925	0.0055	0.283270	0.000007	WRZ Pic	1.00	31.2	13.3	2.71
9805	18.2988	0.0031	15.4721	0.0027	38.0453	0.0067	0.283325	0.000011	WRZ Pic	-0.25	29.5	17.8	3.80
9806	18.6014	0.0015	15.5024	0.0013	38.2919	0.0032	0.283222	0.000007	WRZ Pic	-0.50	17.6	17.4	2.29
9809	18.3684	0.0061	15.4715	0.0054	38.0646	0.0133	0.283356	0.000009	WRZ Pic	-1.06	23.0	16.5	4.70
9810	18.7508	0.0009	15.5006	0.0008	38.3672	0.0019	0.283186	0.000005	WRZ Bas	-2.30	7.04	18.2	1.03
9812	18.4497	0.0041	15.4838	0.0016	38.1496	0.0003	0.283302	0.000007	WRZ Pic	-0.72	21.7	12.6	3.13
9815	18.8719	0.0010	15.5175	0.0009	38.4693	0.0025	0.283175	0.000006	WRZ Bas	-1.92	2.62	13.2	1.41
9101	18.5398	0.0017	15.4870	0.0015	38.2243	0.0039	0.283217	0.000008	WRZ Pic	-1.37	18.3	11.6	3.80

Table 2: Abundances (in ppb) of highly siderophile elements (HSE) in a suite of Icelandic high-MgO lavas. Also included are data for a chromite (Crt) and olivine (Ol) separate from the sample ICE-4A. Rhenium and Os abundances have previously been reported in Brandon et al. (2007). n. d. – not determined.

Samples	MgO (wt.%)	Os	Ir	Ru	Pt	Pd	Re
ICE-0	20.1	0.863	0.462	1.77	9.98	22.8	0.612
ICE-2	20.7	1.05	0.511	1.58	7.07	13.1	0.306
ICE-3	18	0.124	0.153	0.420	3.26	4.63	0.356
ICE-4A	25.3	0.457	0.311	1.37	4.40	7.20	0.494
ICE-4A Ol	n.d.	0.313	0.266	1.74	2.47	0.264	n.d.
ICE-4A Crt	n.d.	31.4	19.6	104	9.13	5.28	n.d.
ICE-4B	23.9	0.882	0.57	1.21	5.15	7.47	0.616
ICE-5	18.8	0.411	0.695	0.947	6.4	10.4	0.46
ICE-6	12.5	0.14	0.123	0.488	5.49	12.6	0.712
ICE-8A	15.6	0.273	0.152	0.668	1.06	0.987	0.487
ICE-8B	19.3	0.516	0.233	1.07	1.96	0.974	0.28
ICE-9A	13.0	0.148	0.106	0.488	1.39	0.990	0.476
ICE-10	12.3	0.184	0.156	0.520	4.94	6.58	0.432
ICE-11	17.4	0.877	0.376	1.31	6.64	12.9	0.391
9101	22.4	0.746	n.d.	n.d.	n.d.	n.d.	0.253
9805	28.5	1.07	0.524	2.59	9.55	9.76	0.152
9806	15.2	0.674	0.299	1.03	6.49	15.0	0.358
9809	24.8	1.03	0.504	2.64	6.01	9.46	0.337
9810	10.7	0.0630	0.125	0.175	4.28	6.59	0.586
9812	16.0	0.424	0.217	0.965	5.23	11.5	0.496
9815	9.50	0.204	0.124	0.270	4.18	6.69	0.574

Table 3: Highly siderophile element abundances in calculated parental magmas of the Icelandic lavas. Abundances are given in ppb. "Regression parental" is derived from MgO-HSE linear regressions to a parental magma MgO of 17.9 wt.% (From Nicklas et al. 2019) and "2σ" is the 95% confidence interval on the calculated parental abundances. "Olivine parental" and "Chromite parental" are calculated from the ICE-4A olivine and chromite separates listed in **Table 2** using published partition coefficients (Puchtel and Humayun 2001). Also listed is the average abundances in the three EVZ lavas, and the 2 standard deviations (2SD) on that average. See text for further details.

	Regression Parental	2σ	Olivine Parental	Chromite Parental	Average EVZ	2SD
Re	0.44	0.32			0.41	0.23
Pd	10.4	10.3	8.80	3.30	0.98	0.02
Pt	5.20	4.21	30.9	2.77	1.47	0.91
Ru	1.09	0.28	1.02	0.69	0.74	0.60
Ir	0.31	0.14	0.35	0.20	0.16	0.13
Os	0.67	0.27	0.35	0.21	0.31	0.37

Figure Captions

Figure 1: $\varepsilon^{143}Nd$ plotted against $\varepsilon^{176}Hf$ for the sample set, using the chondritic uniform reservoir (CHUR) values of Bouvier et al. (2008). Line is the terrestrial mantle Hf-Nd array of Vervoort and Blichert-Toft (1999). Neodymium isotope data for our sample set are from Brandon et al. (2007). Literature Nd and Hf isotopic data are from Kempton et al. (2000); Stracke et al. (2003); and Peate et al. (2010). Lit – literature data.

Figure 2: Whole-rock $^{206}Pb/^{204}Pb$, $^{208}Pb/^{204}Pb$ and $^{176}Hf/^{177}Hf$ ratios plotted against $^{3}He/^{4}He$ ratios (in R_A, which is the ratio of samples to air) determined on olivine separates, for the sample set. Helium isotopic data are from Brandon et al. (2007).

Figure 3: Plots of $^{143}Nd/^{144}Nd$, $^{176}Hf/^{177}Hf$, $^{87}Sr/^{86}Sr$, $^{206}Pb/^{204}Pb$, $^{207}Pb/^{204}Pb$ and $^{208}Pb/^{204}Pb$ ratios against $^{187}Os/^{188}Os$ ratios for the dataset. Osmium and Nd isotope data are from Brandon et al. (2007), and Sr isotope data are from Debaille et al. (2009).

Figure 4: Whole-rock double spike-corrected Pb isotopic ratios of Icelandic rift zone lavas. Mixing end-members (IE1, IE2, ID1, ID2) are from Thirlwall et al. (2004). Literature data are from Baker et al. (2004); Thirlwall et al. (2004); Peate et al. (2009); (2010) and Manning and Thirlwall, (2014). Lit-literature data. Solid line is the Northern Hemisphere Reference Line (NHRL) of Hart (1986).

Figure 5a: Primitive mantle (PM) normalized (Day et al. 2017) abundances of the HSE in the studied samples. **b:** PM-normalized HSE abundances of bulk rock powder of the WVZ picrite ICE-4A as well as olivine and chromite mineral separates of the same sample.

Figure 6a: Abundances of Pd (in ppb) plotted against $^{206}Pb/^{204}Pb$ showing a negative correlation. **b:** Abundances of MgO (in wt.%) plotted against $^{206}Pb/^{204}Pb$ also showing a broad negative correlation

Figure 7a: Estimated PM normalized (Day et al. 2017) parental magma HSE patterns of Icelandic lavas. "Regression Parental" is calculated using linear regression of the bulk rock samples, while "Olivine Parental" and "Chromite Parental" are calculated using liquid-mineral partition coefficients taken from Puchtel and Humayun (2001). The "Average EVZ" is the mean pattern of the three EVZ bulk rocks and show notably depleted Pd and Pt concentrations compared to the other parental magmas. See text for more details. **b.** Iceland "Regression Parental" compared to calculated parental lavas for other OIB volcanos, Hawaii data are from Ireland et al. (2009); Canary Islands data are from Day et al. (2010) and Azores data are from Waters et al. (2020).

Figure 8: Whole-rock double spike-corrected $\Delta^{207}Pb$ and $\Delta^{208}Pb$ of Icelandic rift zone lavas. $\Delta^{207}Pb$ and $\Delta^{208}Pb$ are defined as the vertical deviation of data points from the NHRLs of Hart (1986) in $^{206}Pb/^{204}Pb$-$^{207}Pb/^{204}Pb$ and $^{206}Pb/^{204}Pb$-$^{208}Pb/^{204}Pb$ plots respectively, as shown in **Fig. 4.** Mixing endmembers (IE1, IE2, ID1, ID2) are from Thirwall et al. (2004). Literature data are from the same sources as **Fig. 4**. Lit-literature data.

References Cited

Baker J., Peate D., Waight T., Meyzen C. (2004). Pb isotopic analysis of standards and samples using a ^{207}Pb-^{204}Pb double spike and thallium to correct for mass bias with a double-focusing MC-ICP-MS. *Chemical Geology* **211**: 275-303.

Barnes S.-J., Naldrett A. J., Gorton M. P. (1985). The Origin of the Fractionation of Platinum-Group Elements in Terrestrial Magmas. **53**(3-4): 303-323.

Bizimis M., Sen G., Salters V. J. M., Keshav S. (2005). Hf-Nd-Sr isotope systematics of garnet pyroxenites from Salt Lake Crater, Oahu, Hawaii: Evidence for a depleted component in Hawaiian volcanism. *Geochimica et Cosmochimica Acta* **69**(10): 2629-2646.

Bizimis M., Sen G., Salters V. J. M. (2003). Hf-Nd isotope decoupling in the oceanic lithosphere constraints from spinel peridotite from Oahu, Hawaii. *Earth and Planetary Science Letters* **217**: 43-58.

Blichert-Toft J., Argranier A., Andres M., Kingsley R., Schilling J.-G. (2005). Geochemical segmentation of the Mid-Atlantic Ridge north of Iceland and ridge-hot spot interaction in the North Atlantic. *Geochem. Geophys. Geosyst.* **6**(1): Q01E19.

Blichert-Toft J., Frey F. A., Albarede F. (1999). Hf Isotope Evidence for Pelagic Sediments in the Source of Hawaiian Basalts. *Science* **285**: 879-882.

Brandon A. D., Graham D. W., Waight T., Gautason B. (2007) ^{186}Os and ^{187}Os enrichments and high-$^{3}He/^{4}He$ sources in the Earth's mantle: Evidence from Icelandic picrites. *Geochimica et Cosmochimica Acta* **71**: 4570-4591.

Brandon A. D., Walker R. J., Morgan J. W., Norman M. D., Prichard H. M. (1998). Coupled ^{186}Os and ^{187}Os Evidence for Core-Mantle Interaction. *Science* **280**(5369): 1570-1573.

Brett E. K. A., Prytulak J., Rehkamper M., Hammond S. J., Chauvel C., Stracke A., Willbold M. (2021). Thallium elemental and isotopic systematics in ocean island lavas. *Geochimica et Cosmochimica Acta* (in press).

Bouvier A., Vervoort J. D., Patchett J. D. (2008). The Lu-Hf and Sm-Nd isotopic composition of CHUR: Constraints from unequilibrated chondrites and implications for the bulk composition of terrestrial planets. *Earth and Planetary Science Letters* **273**: 48-57.

Chauvel C., Hemond C. (2000). Melting of a complete section of recycled oceanic crust: Trace element and Pb isotopic evidence from Iceland. *Geochem. Geophys. Geosys.* **1**(1).

Condomines M., Gronvold K., Hooker P. J., Muehlenbachs K., O'Nions R. K., Oskarsson N., Oxburgh E. R. (1983). Helium, oxygen, strontium, and neodymium isotopic relationships in Icelandic Volcanics. *Earth and Planetary Science Letters* **66** 125-136.

Day J. M. D., Walker R. J., Warren J. M. (2017). ^{186}Os-^{187}Os and highly siderophile element abundance systematics of the mantle revealed by abyssal peridotites and Os-rich alloys. *Geochimica et Cosmochimica Acta* **200**: 232-254.

Day J. M. D., Barry P. H., Hilton D. R., Pearson D. G., Burgess, R., Taylor L. A. (2015) The helium flux from the continents and ubiquity of low-$^{3}He/^{4}He$ recycled crust and lithosphere. *Geochimica et Cosmochimica Acta,* 153, 116-133.

Day J. M. D. (2013) Hotspot volcanism and highly siderophile elements. *Chemical Geology* **341**: 50-74.

Day J. M. D., Pearson D. G., Macpherson C. G., Lowry D., Carracedo J. C. (2010). Evidence for distinct properties of subducted crust and lithosphere in HIMU-type mantle beneath El Hierro and La Palma, Canary Islands. *Geochimica et Cosmochimica Acta* **74**: 6565-6589.

Debaille V., Tronnes R. G., Brandon A. D., Waight T. E., Graham D. W., Lee C.-T. A. (2009). Primitive off-rift basalts from Iceland and Jan Mayen: Os-isotopic evidence for a mantle source containing enriched subcontinental lithosphere. *Geochimica et Cosmochimica Acta* **73**: 3423-3449.

Doucelance R., Escrig S., Moreira M., Gariepy C., Kurz M. D. (2003). Pb-Sr-He isotope and trace element geochemistry of the Cape Verde Archipelago. *Geochimica et Cosmochimica Acta* **67**(19): 3717-3733.

Eiler J. M., Farley K. A., Stolper E. M. (1998). Correlated helium and lead isotope isotope variations in Hawaiian lavas. *Geochimica et Cosmochimica Acta* **62**: 1977-1984.

Eisele J., Sharma M., Galer S. J. G., Blichert-Toft J., Devey C. W., Hofmann A. W. (2002). The role of sediment recycling in EM-1 inferred from Os, Pb, Hf, Nd, Sr isotope and trace element systematics of the Pitcairn hotspot. *Earth and Planetary Science Letters* **196**: 197-212.

Ellam R. M., Stuart F. M. (2004). Coherent He-Nd-Sr isotope trends in high $^{3}He/^{4}He$ basalts: implications for a common reservoir, mantle heterogeneity and convection. *Earth and Planetary Science Letters* **228**: 511-523.

Fitton J. G., Saunders A. D., Kempton P. D., Hardarson B. S. (2003). Does depleted mantle form an intrinsic part of the Iceland plume? *Geochem. Geophys. Geosys.* **4**(3).

Fitton J. G., Saunders A. D., Norry M. J., Hardarson B. S., Taylor R. N. (1997). Thermal and chemical structure of the Iceland plume. *Earth and Planetary Science Letters* **153**: 197-208.

Hanan B. B., Blichert-Toft J., Kingsley R., Schilling J.-G. (2000). Depleted Iceland mantle plume geochemical signature: Artifact of multicomponent mixing? *Geochem. Geophys. Geosys.* **1**(1).

Hardardottir S., Halldorsson S. A., Hilton D. R. (2018). Spatial distribution of helium isotopes in Icelandic geothermal fluids and volcanic materials with implications for location, upwelling and evolution of the Icelandic mantle plume. *Chemical Geology* **480**: 12-27.

Hart S. R. (1984). A large-scale isotope anomaly in the Southern Hemisphere mantle. *Nature* **309**: 753-757.

Hemond C., Arndt N. T., Lichtenstein U., Hofmann A. W., Askarsson N. and Steinthorsson S. (1993) The heterogeneous Iceland plume: Nd–Sr–O isotopes and trace element constraints. *J. Geophys. Res.* **98**, 15833–15850.

Hilton D. R., Gronvold K., Macpherson C. G., Castillo P. R. (1999). Extreme $^{3}He/^{4}He$ ratios in northwest Iceland: constraining the common component in mantle plumes. *Earth and Planetary Science Letters* **173**: 53-60.

Hofmann A. W. (1997). Mantle geochemistry: the message from oceanic volcanism. *Nature* **385**: 219-229.

Ireland T. J., Walker R. J., Garcia M. O. (2009). Highly siderophile element and ^{187}Os isotope systematics of Hawaiian picrites: Implications for parental melt composition and source heterogeneity. *Chemical Geology* **260**: 112-128.

Jackson M. G., Blichert-Toft J., Halldorsson S. A., Mundl-Petermeier A., Bizimis M., Kurz M. D., Price A. A., Hardardottir S., Willhite L. N., Breddam K., Becker T. W., Fischer R. A. (2020). Ancient helium and tungsten isotopic signatures preserved in mantle domains least modified by crustal recycling. *PNAS* **117**(49): 30993-31001.

Kelley K. A., Plank T., Farr L., Ludden J., Staudigel H. (2005). Subduction cycling of U, Th, and Pb. *Earth and Planetary Science Letters* **234**: 369-383.

Kempton P. D., Fitton J. G., Saunders A. D., Nowell G. M., Taylor R. N., Hardarson B. S. Pearson G. (2000). The Iceland plume in space and time: a Sr-Nd-Pb-Hf study of the North Atlantic rifted margin. *Earth and Planetary Science Letters* **177**: 255-271.

Kokfelt T. F., Hoernle K., Hauff F., Fiebig J., Werner R., Garbe-Schonberg D. (2006). Combined Trace Element and Pb-Nd-Sr-O Isotope Evidence for Recycled Oceanic Crust (Upper and Lower) in the Iceland Mantle Plume. *J. Petrol.* **47**(9): 1705-1749.

Koornneef J. M., Stacke A., Bourdon B., Meier M. A., Jochum K. P., Stoll B., Gronvold K. (2012). Melting of a Two-component Source beneath Iceland. *J. Petrol.* **53**(1): 127-157.

Kurz M. D., Meyer P. S., Sigurdsson H. (1985). Helium isotopic systematics within the neovolcanic zones of Iceland. *Earth and Planetary Science Letters* **75**: 291-305.

Luguet A., Pearson D. G., Nowell G. M., Dreher S. T., Coggon J. A., Spetsius Z. V., Parman S. W. (2008). Enriched Pt-Re-Os Isotope Systematics in Plume Lavas Explained by Metasomatic Sulfides. *Science* **319**: 453-456.

Macpherson C. G., Hilton D. R., Day J. M. D., Lowry D., Gronvold K. (2005). High-$^{3}He/^{4}He$, depleted mantle and low-$\delta^{18}O$, recycled oceanic lithosphere in the source of central Iceland magmatism. *Earth and Planetary Science Letters* **233**: 411-427.

Manning C. J., Thirlwall M. F. (2014). Isotopic evidence for interaction between Oraefajokull mantle and the Eastern Rift Zone, Iceland. *Contrib. Mineral. Petrol.* **167**(1): 1-22.

Momme P., Oskarsson N., Keays R. R. (2003). Platinum-group elements in the Icelandic rift system: melting processes and mantle sources beneath Iceland. *Chemical Geology* **196**: 209-234.

Mundl A., Touboul M., Jackson M. G., Day J. M. D., Kurz M. D., Lekic V., Helz R. T., Walker R. J. (2017). Tungsten-182 heterogeneity in modern ocean island basalts. *Science* **356**: 66-69.

Nicklas R. W., Puchtel I. S., Ash R. D., Piccoli P. M., Hanski E., Nisbet E. G., Waterton P, M., Pearson D. G., Anbar A. D. (2019) Secular mantle oxidation across the Archean-Proterozoic boundary: evidence from V partitioning in komatiites and picrites. *Geochimica et Cosmochimica Acta* **250**: 49-75.

Nielsen S. G., Rehkämper M., Brandon A. D., Norman M. D., Turner S., O'Reilly S. Y. (2007). Thallium isotopes in Iceland and Azores lavas – Implications for the role of altered crust mantle geochemistry. *Earth and Planetary Science Letters* **264**: 332-345.

Peate D. W., Breddam K., Baker J. A., Kurz M. D., Barker A. K., Prestvik T., Grassineau N., Skovgaard A. C. (2010). Compositional characteristics and spatial distribution of enriched Icelandic mantle components. *J. Petrol.* **51**(7): 1447-1475.

Peate D. W., Baker J. A., Jakobsson S. P., Waight T. E., Kent A. J. R., Grassineau N. V., Skovgaard A. C. (2009). Historic magmatism on the Reykjanes Peninsula, Iceland: a snap-shot of melt generation at a ridge segment. *Contrib. Mineral. Petrol.* **157**: 359-382.

Porcelli D., Halliday A. N. (2001). The core as a possible source of mantle helium. *Earth and Planetary Science Letters* **192:** 45-56.

Prestvik T., Goldberg S., Karlsson H., Grönvold K. (2001). Anomalous strontium and lead isotope signatures in the off-rift Öræfajökull central volcano in south-east Iceland: Evidence for enriched endmember(s) of the Iceland mantle plume? *Earth and Plaentary Science Letters* **190**: 211-220.

Puchtel I.S., Humayun M., Campbell A.J., Sproule R.A., Lesher C.M. **(2004)** Platinum group element geochemistry of komatiites from the Alexo and Pyke Hill areas, Ontario, Canada. *Geochimica et Cosmochimica Acta* **68**: 1361-1383.

Puchtel I.S., Humayun M. (2005) Highly siderophile element geochemistry of ^{187}Os-enriched 2.8-Ga Kostomuksha komatiites, Baltic Shield. *Geochimica et Cosmochimica Acta* **69**: 1607-1618.

Puchtel I. S., Humayun M. (2001). Platinum group element fractionation in a komatiitic basalt lava lake. *Geochimica et Cosmochimica Acta* **65**: 2979-2993.

Puchtel I.S., Blichert-Toft J., Touboul M., Walker R.J., Nisbet E.G., Byerly G., Anhaeusser C. (2013) Insights into early Earth from Barberton komatiites: Evidence from lithophile isotope and trace element systematics. *Geochimica et Cosmochimica Acta* **108:** 63-90.

Puchtel I.S., Blichert-Toft J., Touboul M., Horan M.F., Walker R.J. (2016) The Coupled ^{182}W-^{142}Nd Record of the Early Terrestrial Mantle Differentiation. *Geochemistry, Geophysics, Geosystems* **17**: 2168-2193.

Rehkämper M., Halliday A. N., Fitton J. G., Lee D.-C., Wieneke M., Arndt N. T. (1999). Ir, Ru, Pt, and Pd in basalts and komatiites: New constraints for the geochemical behavior of the platinum-group elements in the mantle. *Geochimica et Cosmochimica Acta* **63**(22): 3915-3934.

Shorttle O., Maclennan J. (2011). Compositional trends of Icelandic basalts: Implications for short-length scale lithological heterogeneity in mantle plumes. *Geochem. Geophys. Geosys.* **12**(11).

Stracke A., Genske F., Berndt J., Koornneef J. M. (2019). Ubiquitous ultra-depleted domains in Earth's mantle. *Nature Geoscience* **12**: 851-855.

Stracke A., Snow J. E., Hellebrand E., von der Handt A., Bourdon B., Birbaum K., Gunther D. (2011). Abyssal peridotite Hf isotopes identify extreme mantle depletion. *Earth and Planetary Science Letters* **308**: 359-368.

Stracke A., Zindler A., Salters V. J. M., McKenzie D., Blichert-Toft J., Albarede F., Gronvold K. (2003). Theistareykir revisited. *Geochem. Geophys. Geosys.* **4**(2).

Thirlwall M. F., Gee M. A. M., Lowry D., Mattey D. P., Murton B. J., Taylor R. N. (2006). Low $\delta^{18}O$ in the Icelandic mantle and its origins: Evidence from Reykjanes Ridge and Icelandic lavas. *Geochimica et Cosmochimica Acta* **70**: 993-1019.

Thirlwall M. F., Gee M. A. M., Taylor R. N., Murton B. J. (2004). Mantle components in Iceland and adjacent ridges investigated using double-spike Pb isotope ratios. *Geochimica et Cosmochimica Acta* **68**(2): 361-386.

Thirlwall M. F. (2002). Multicollector ICP-MS analysis of Pb isotopes using a ^{207}Pb-^{204}Pb double spike demonstrates up to 400 ppm/amu systematics errors in Tl-normalization. *Chemical Geology* **184**: 255-279.

Thirlwall M. F. (1997). Pb isotopic and elemental evidence for OIB derivation from young HIMU mantle. *Chemical Geology* **139**: 51-74.

Thirlwall M. F. (1995). Generation of the Pb isotope characteristics of the Iceland plume. *J. Geo. Soc. London* **152**: 991-996.

Torsvik T. H., Amundsen H. E. F., Tronnes R. G., Doubrovine P. V., Gaina C., Kusznir N. J., Steinberger B., Corfu F., Ashwal L. D., Griffin W. L., Werner S. C., Jamtveit B. (2015). Continental crust beneath southeast Iceland. *PNAS* **112**(15): 1818-1827.

Ulfbeck D., Baker J., Waight T., Krogstad E. (2003). Rapid sample digestion by fusion and chemical separation of Hf for isotopic analysis by MC-ICPMS. *Talanta* **59**: 365-373.

Vervoort J. D., Blichert-Toft J. (1999). Evolution of the depleted mantle: Hf isotope evidence from juvenile rocks through time. *Geochimica et Cosmochimica Acta* **63**(3-4): 533-556.

Zindler A., Hart S. (1986) Chemical Geodynamics. *Ann. Rev. Earth Planet. Sci.* **14**: 493-571.

Figure 1.

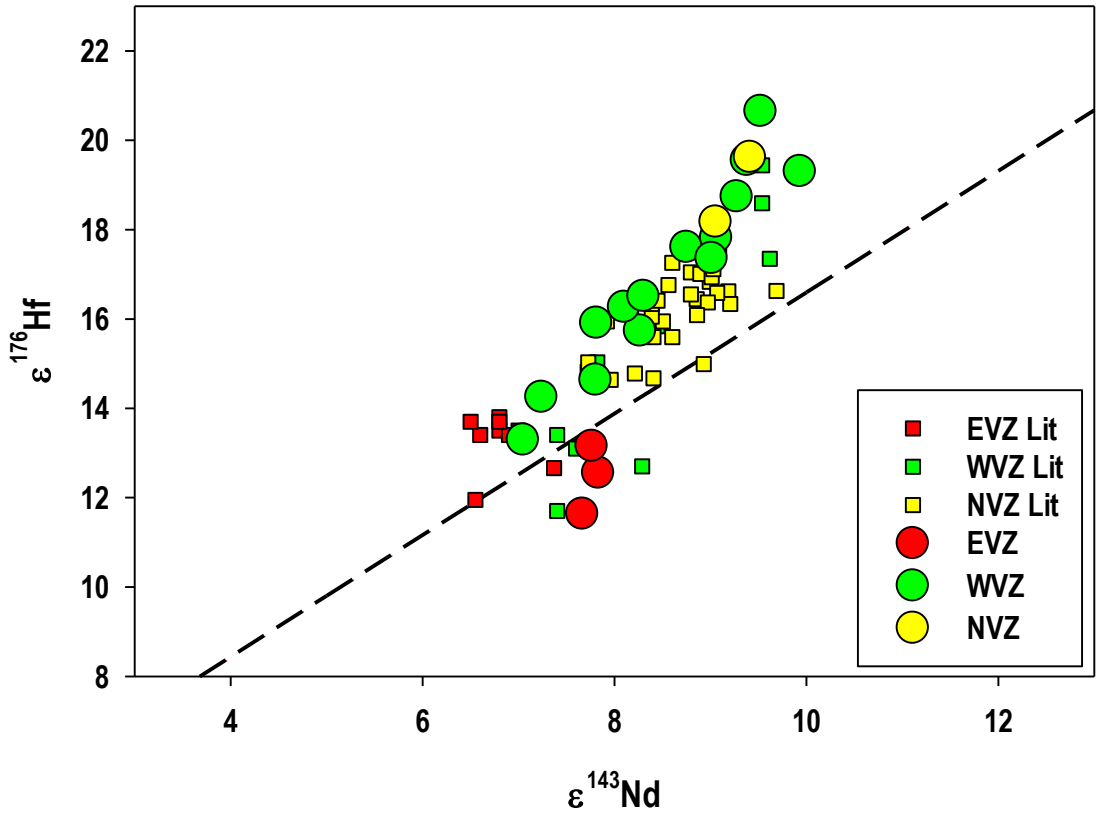
22
20
18
16
14
12
10
8
4
6
8
10
12
ε176Hf
ε143Nd
EVZ Lit
WVZ Lit
NVZ Lit
EVZ
WVZ
NVZ

Figure 2.

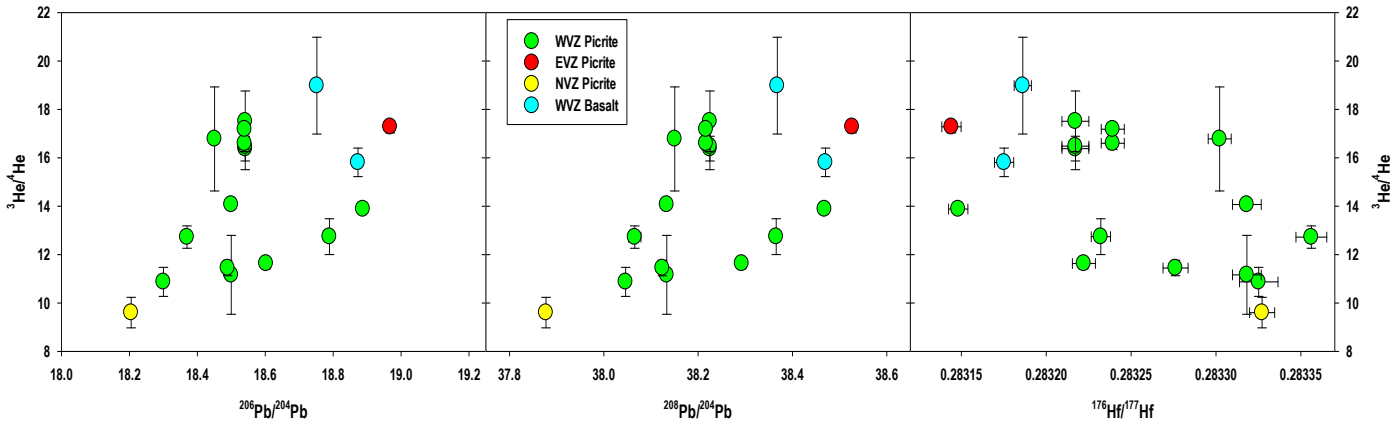
WVZ Picrite
EVZ Picrite
NVZ Picrite
WVZ Basalt
$^{3}He/^{4}He$
$^{206}Pb/^{204}Pb$
$^{208}Pb/^{204}Pb$
$^{176}Hf/^{177}Hf$

Figure 3.

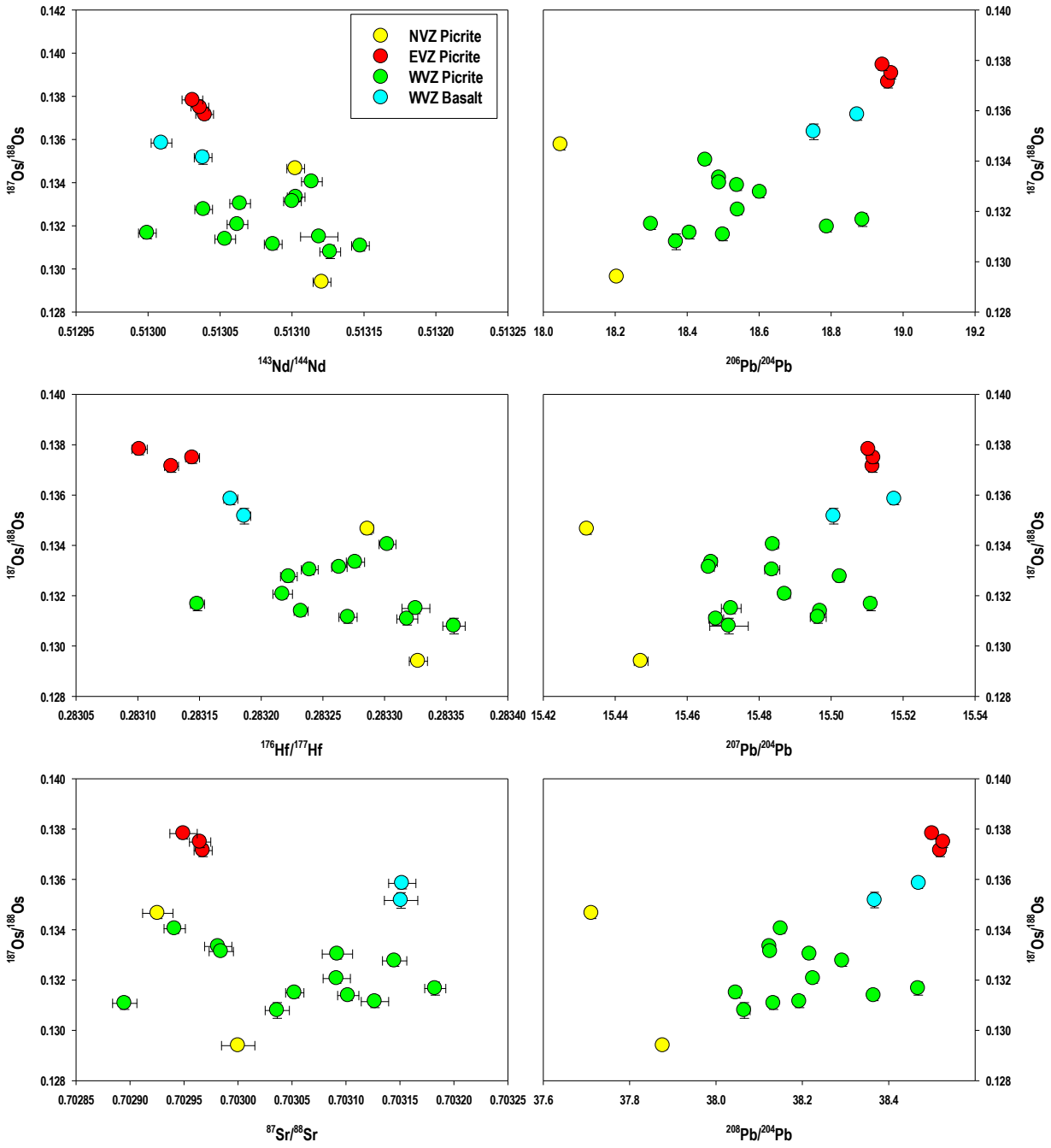
NVZ Picrite
EVZ Picrite
WVZ Picrite
WVZ Basalt
$^{187}Os/^{188}Os$
$^{143}Nd/^{144}Nd$
$^{206}Pb/^{204}Pb$
$^{176}Hf/^{177}Hf$
$^{207}Pb/^{204}Pb$
$^{87}Sr/^{88}Sr$
$^{208}Pb/^{204}Pb$

Figure 4.

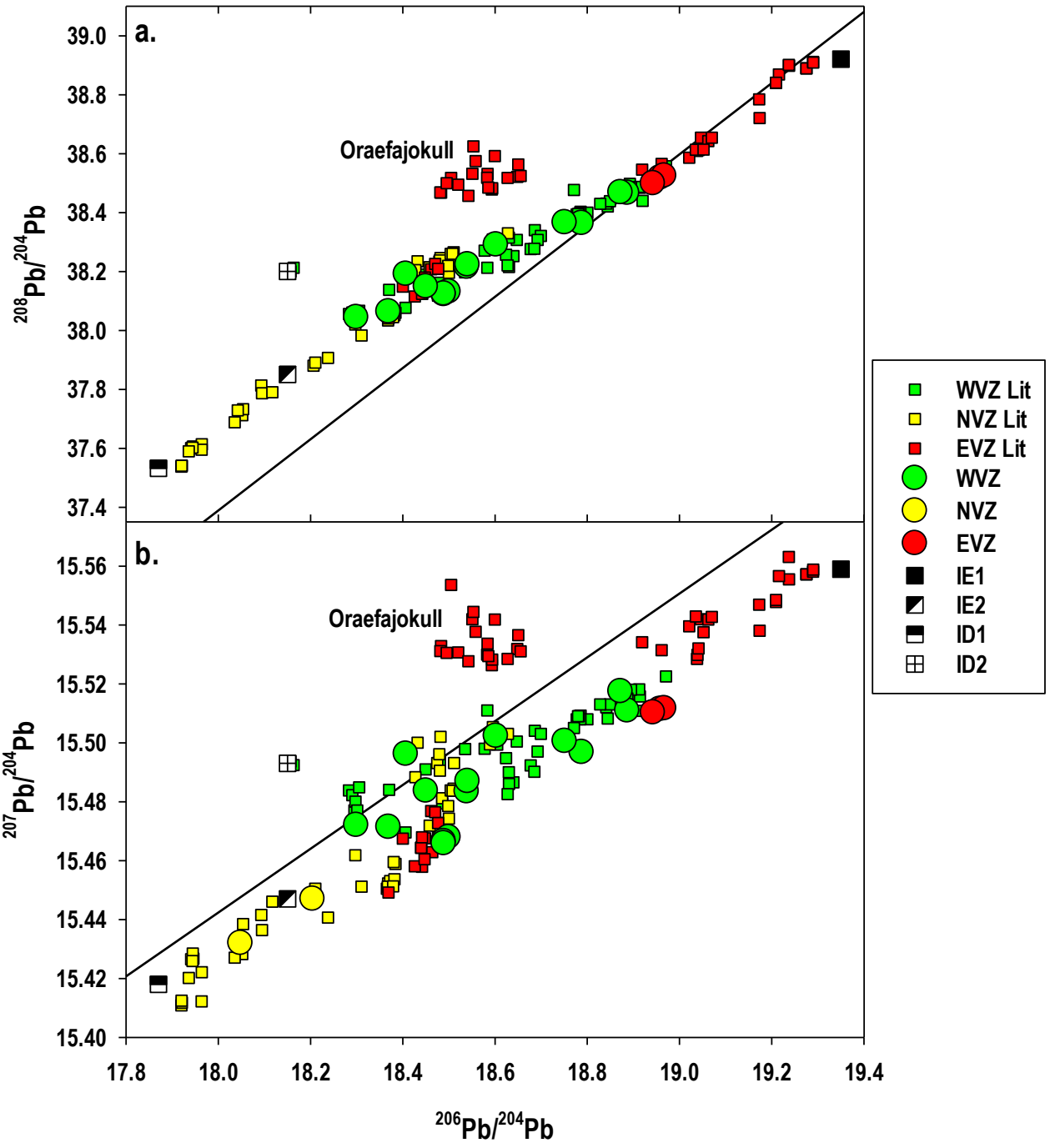
a.
b.
Oraefajokull
Oraefajokull
$^{208}Pb/^{204}Pb$
$^{207}Pb/^{204}Pb$
$^{206}Pb/^{204}Pb$
39.0
38.8
38.6
38.4
38.2
38.0
37.8
37.6
37.4
15.56
15.54
15.52
15.50
15.48
15.46
15.44
15.42
15.40
17.8
18.0
18.2
18.4
18.6
18.8
19.0
19.2
19.4
WVZ Lit
NVZ Lit
EVZ Lit
WVZ
NVZ
EVZ
IE1
IE2
ID1
ID2

Figure 5.

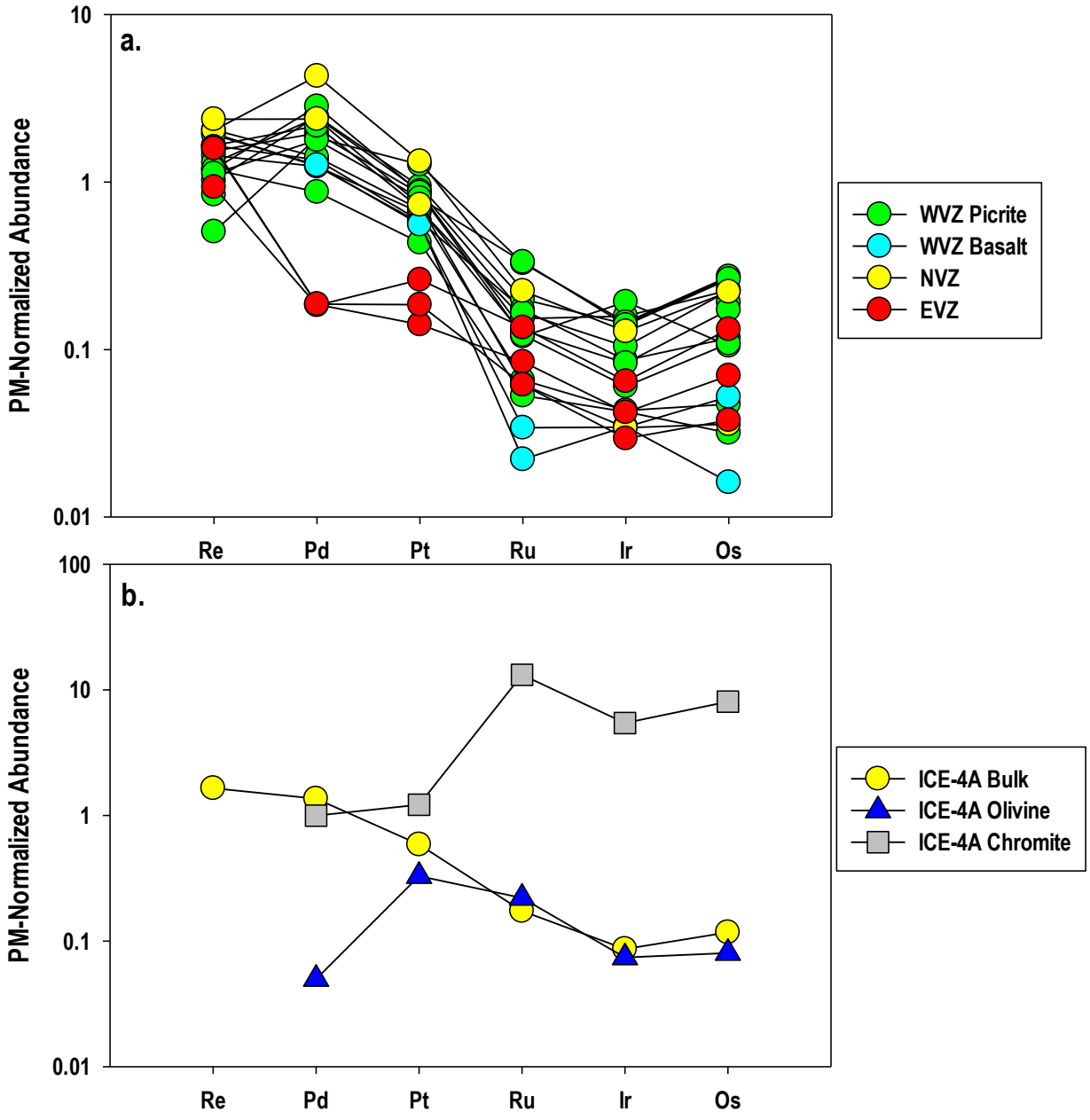
a.
PM-Normalized Abundance
10
1
0.1
0.01
Re
Pd
Pt
Ru
Ir
Os
WVZ Picrite
WVZ Basalt
NVZ
EVZ
b.
PM-Normalized Abundance
100
10
1
0.1
0.01
Re
Pd
Pt
Ru
Ir
Os
ICE-4A Bulk
ICE-4A Olivine
ICE-4A Chromite

Figure 6.

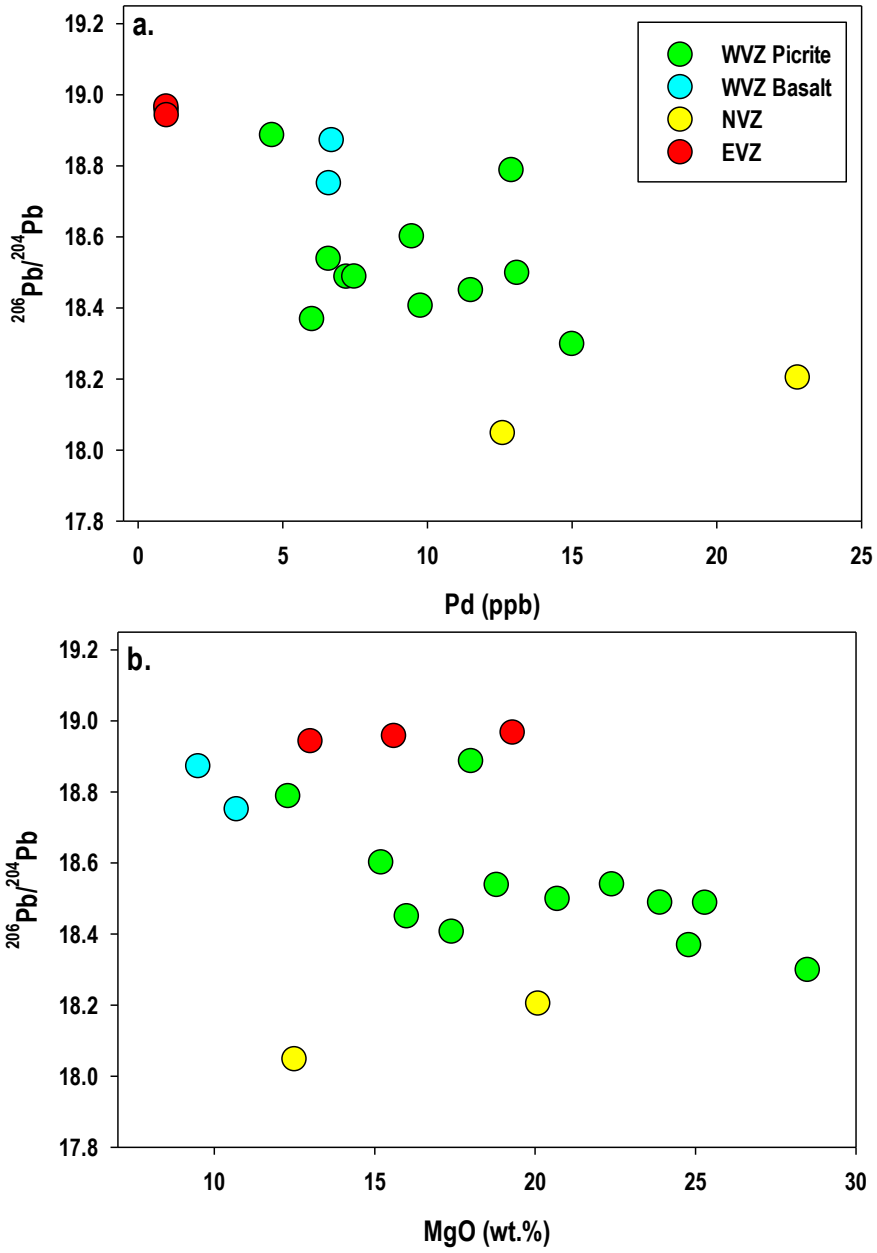
a.
WVZ Picrite
WVZ Basalt
NVZ
EVZ
$^{206}Pb/^{204}Pb$
Pd (ppb)
b.
$^{206}Pb/^{204}Pb$
MgO (wt.%)

Figure 7.

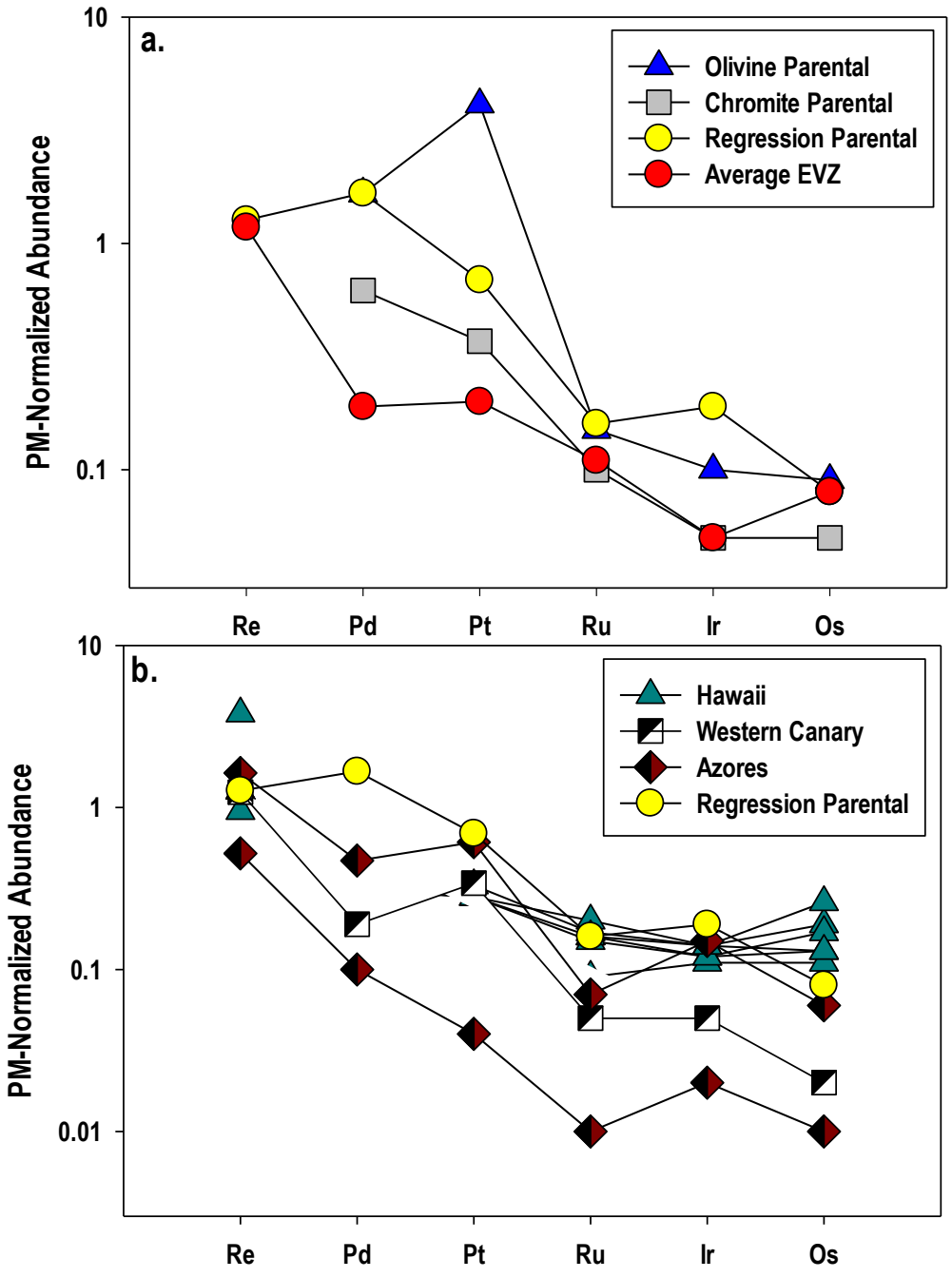
a.
Olivine Parental
Chromite Parental
Regression Parental
Average EVZ
PM-Normalized Abundance
10
1
0.1
Re
Pd
Pt
Ru
Ir
Os
b.
Hawaii
Western Canary
Azores
Regression Parental
PM-Normalized Abundance
10
1
0.1
0.01
Re
Pd
Pt
Ru
Ir
Os

Figure 8.

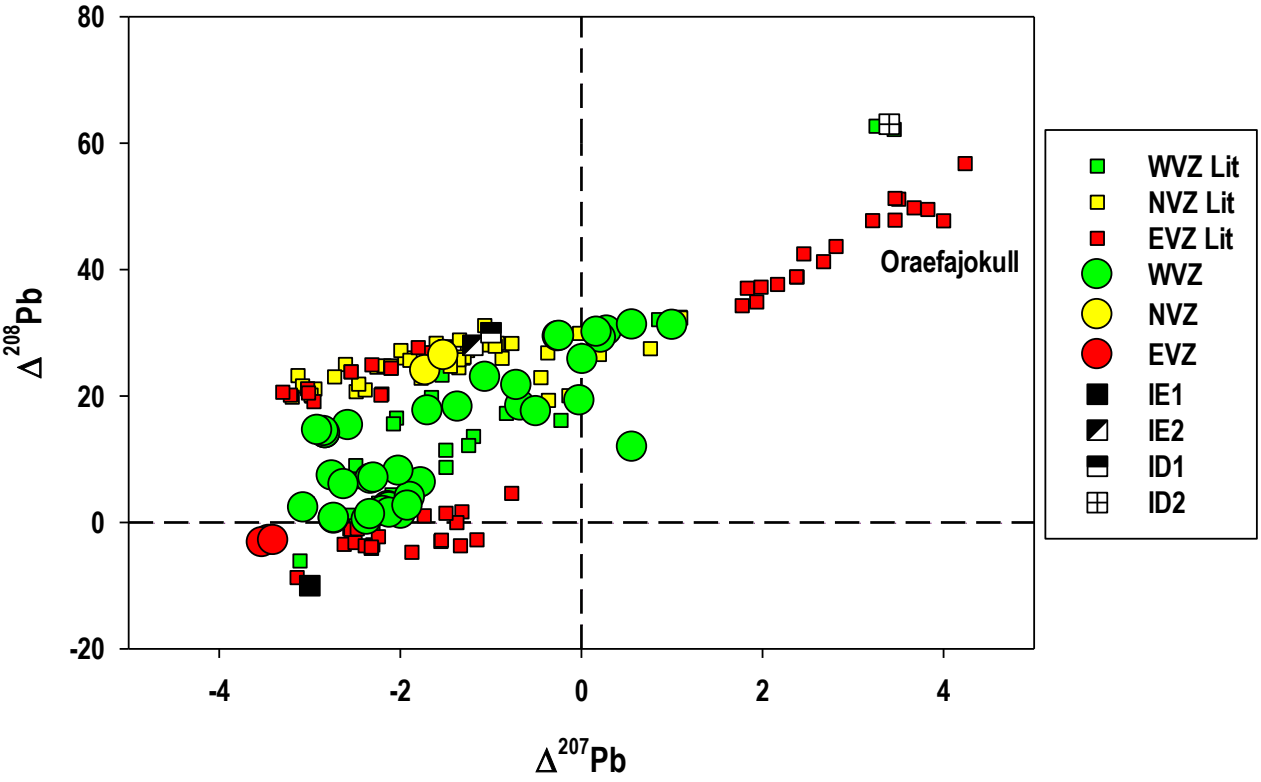
80
60
40
20
0
-20
-4
-2
0
2
4
Δ208Pb
Δ207Pb
Oraefajokull
WVZ Lit
NVZ Lit
EVZ Lit
WVZ
NVZ
EVZ
IE1
IE2
ID1
ID2